Olefin Polymerization Promoted by a Stereorigid Bridged Diiminobis(phenolate) Zirconium Complex[†]

Cinzia Cuomo,[‡] Maria Strianese,[‡] Tomás Cuenca,[§] Martial Sanz,[§] and Alfonso Grassi*,[‡]

Dipartimento di Chimica, Università di Salerno, 84081 Baronissi, Italy, and Departamento de Química Inorgánica, Universidad de Alcalá, Campus Universitario, Edificio de Farmacia, 28871 Alcalá de Henares, Spain

ABSTRACT: Two diiminobis(phenolate) zirconium complexes [C$_6$H$_{10}$-{N=CH-(3,5-^{t}Bu$_2$C$_6$H$_2$-2-O)-κO}$_2$]-ZrX$_2$ [X = CH$_2$Ph (**1**), Cl (**3**)] have been synthesized and characterized by NMR solution spectroscopy. Complex **1** was found conformationally stable and isolated in the octahedral C_2 symmetric form. When exposed to the light in hydrocarbon solution, **1** readily undergoes to 1,2 benzyl migration converting the diiminobis(phenolate) ligand in the corresponding benzylamidoiminobis(phenolate). Complex **3** is more thermally stable and found in slow equilibrium between the cis-α and cis-β forms with the former largely prevalent (9:1 molar ratio). The rate of interconversion between the two diastereoisomers was estimated in 3.6 × 10^{-1} s^{-1} by NMR exchange spectroscopy (EXSY). **1** and **3** are active ethylene polymerization catalysts after reaction with MAO or [CPh$_3$][B(C$_6$F$_5$)$_4$]/Al-^{i}Bu$_3$. The polydispersity index of polyethylene produced by **1** is about 2, suggesting the presence of a single active species and that the symmetry of the precatalyst is retained during polymerization. The catalyst is stable over 3 h, and the polymerization activity linearly increases with time. Copolymers of ethylene with propylene or 1-hexene were synthesized, and the ^{13}C NMR analysis of their microstructure suggested the highly regioregular 1,2 insertion of the 1-olefin and the inability of the ligand environment to express stereochemical control during monomer insertion.

1. Introduction

Despite the efforts devoted over the past two decades by scientists of industrial and academic teams in the field of homogeneous olefin polymerization catalysis, the performances of the heterogeneous Ziegler−Natta catalysts in isotactic specific polymerization of 1-olefins are still unequaled. The discovery of the group 4 metallocene catalysts permitted a deep knowledge of the olefin polymerization mechanism and the synthesis of novel polymers as syndiotactic, hemi-isotactic, or stereo-block polypropylene.[1−4] However, the polymerization activity and the stereo- and regiospecificity of the heterogeneous Ziegler−Natta catalysts are still the highest, and the search for novel homogeneous catalysts mimicking the behavior of the active sites on the surface of the heterogeneous Ziegler−Natta catalysts is thus a topic of current interest.

Group 4 metal complexes in octahedral environment have been synthesized using different ligand sets in order to get the appropriate symmetry and steric hindrance at the metal center to produce the desired site controlled stereospecific olefin polymerization.

Eisen claimed the synthesis of isotactic poly(1-hexene) and polypropylene via the enantiomorphic site controlled mechanism using racemic C_2 symmetric bis-(amidinate) zirconium complexes.[5,6]

Kol obtained zirconium complexes with the same symmetry properties using the diamine bis(phenolate) ligand: isospecific living 1-hexene polymerization was successfully obtained,[7−10] and the steric hindrance at the ortho position of the phenoxo ligand was found critical for the living properties and stereospecificity of the catalyst. Propylene polymerization catalyzed by the same complexes proceeds via highly isospecific primary insertion of the monomer.[11]

Recently, living olefin polymerization catalysts based on bis(iminophenolate) derivatives of group 4 metals were achieved independently by Fujita et al.[12−15] and Coates et al.[16] The living properties of this new class of titanium-based octahedral olefin polymerization catalysts are very attractive, and syndiotactic polypropylene[17−19] and propylene−ethylene block copolymers were synthesized.[20] Despite the C_2 symmetry of the titanium-based precatalysts, the resulting polypropylene exhibits syndiotactic structure arising from secondary monomer insertion and a chain end controlled mechanism.[18,21] Some recent publications tried to rationalize these results on the basis of QM/MM calculation and proposed a chain end stereocontrol mediated by the site chirality. In the frame of fast $\Lambda-\Delta$ configurational isomerization of the octahedral titanium catalyst it was shown that e.g. the *re*-chain ending would favor by about 5.9 kJ mol^{-1} the formation of the Λ complex which, in turn, dictates the coordination−insertion of propylene with the *si* enantioface (*si*-propylene), with the latter favored by about 7.9 kJ mol^{-1} over the *re*-propylene.[22] This could explain why, despite the C_2 symmetric structure of the precatalysts in the solid state, syndiotactic polypropylene is produced. The QM/MM calculation also showed that, by passing from titanium to zirconium, a complex combination of steric and electronic factors would favor the primary insertion of propylene in the case of zirconium.[23] An experimental comparison of the performances in propylene polymerization of bis(iminophenolate) complexes of zirconium and titanium, namely

---

[‡] Università di Salerno.
[§] Universidad de Alcalá.
* To whom correspondence should be addressed. E-mail: agrassi@unisa.it.
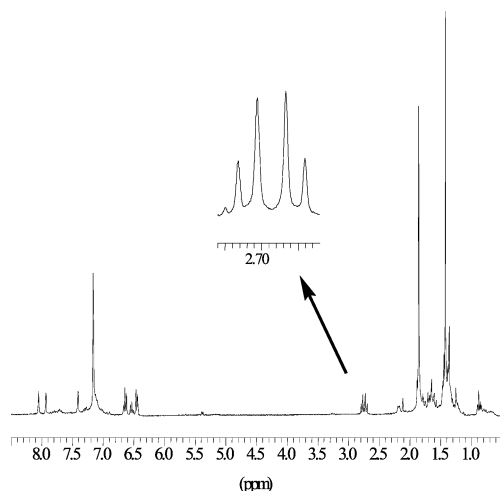
Figure 1. ^{1}H NMR spectrum (C$_6$D$_6$, 25 °C, δ in ppm) of (^{t}Bu$_4$salcyen)ZrBn$_2$ (**1**).

bis[*N*-(3-methylsalicylidene)-2,3,4,5,6-pentafluoroaniline]-MCl$_2$, confirmed the prevailingly primary insertion of propylene with the zirconium-based catalysts (with about 3.5 mol % of regioinversion) where secondary insertion is remarkably favored for titanium.[24] Despite the C_2 symmetry of the zirconium complex in the solid state, the stereospecificity was found poor, and partly syndiotactic polypropylene was obtained.
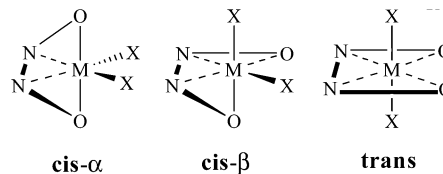
Here we report on the synthesis and catalytic activity in olefin polymerization of stereorigid bridged diiminobis(phenolate) zirconium complexes with C_2 symmetry. In our opinion the presence of the stereorigid bridge would hamper site isomerization during the polymerization process preserving the symmetry of the precatalysts during the polymerization process and yield monomodal, narrow polydispersity of the molecular weight. As a matter of fact, it was previously shown that uni-, bi-, and multimodal polyethylene were produced with bis(iminophenolate) zirconium complexes as a result of the fluxional behavior of the ligand environment.[25]

2. Results and Discussion

2.1. Synthesis of the Ligand and Complexes 1–3. The preligand *N,N*-(1*R*,2*R*)-cyclohexylenebis(3,5-di-*tert*-butylsalicylidene imine) (^{t}Bu$_4$salcyenH$_2$) was synthesized using a modified literature procedure consisting of condensation of 3,5-di-*tert*-butyl-2-hydroxybenzaldehyde with (1*R*,2*R*)-cyclohexanediamine in methanol catalyzed by formic acid.[26,27] The reaction of the preligand with ZrBn$_4$ in toluene at room temperature readily yields the corresponding C_2 symmetric benzyl complex, [C$_6$H$_{10}$-{N=CH-(3,5-^{t}Bu$_2$C$_6$H$_2$-2-O)-κO}$_2$]Zr(CH$_2$Ph)$_2$ [(^{t}Bu$_4$salcyen)ZrBn$_2$, (**1**)] with high selectivity through alkane elimination reaction. The expected product was isolated as a red-orange microcrystalline powder after distillation of the solvent. During the workup a partial decomposition of **1** was monitored by ^{1}H NMR analysis, and the formation of a minor product characterized by a well-defined ^{1}H NMR pattern (see infra for more details) was assessed. When the reaction was repeated in pentane and the manipulation of the reaction solution at room temperature is fast, **1** was isolated analytically pure. The ^{1}H NMR (benzene-d_6, 25 °C) exhibits the typical AB pattern (two doublets at 2.77 and 2.70 ppm; $^2J_{HH}$ = 7.6 Hz; see Figure 1) expected for the diastereotopic methylene protons of the two cis benzyl groups diagnostic of cis-α structure (see Scheme 1). The pres-

ence of two singlets at 1.85 and 1.41 ppm and only one signal at 8.04 ppm for the ^{t}Bu and aldimino groups, respectively, confirms the proposed structure for **1**. The benzyl zirconium complex is stable for months in solid state when stored in a drybox protected from light but in solution is readily, quantitatively, and selectively converted to the imino−amido derivative [C$_6$H$_{10}$-{N=CH-(3,5-^{t}Bu$_2$C$_6$H$_2$-2-O)-κO}{N−CH(CH$_2$Ph)-(3,5-^{t}Bu$_2$C$_6$H$_2$-2-O)-κO,κN}]Zr(CH$_2$Ph) [(Bn^{t}Bu$_4$salcyen)ZrBn, (**2**)] (toluene, 1 day at 25 °C; 90 min at 35 °C) via benzyl migration from zirconium to the imine carbon (Scheme 2). This intramolecular migration was previously observed by Floriani et al.[28] and Scott et al.[29] for the neutral bis(aryliminophenolate)benzyl complexes of titanium and zirconium. A radical mechanism was hypothesized promoted by the presence of a stable radical leaving group (i.e., benzyl): different alkyl complexes bearing e.g. neopentyl groups were found thermally stable for days in solution.[30] A kinetic study of the thermal decomposition of **1** yielding the single product **2** was undertook by ^{1}H NMR spectroscopy at 308 K using the ^{1}H-imine signal and the residual protio signal of benzene-d_6 as reference. The expected first-order kinetics corresponding to the intramolecular 1,2-migration of the benzyl group was actually observed with a specific kinetic constant of 3.6 × 10^{-2} s^{-1} (see Supporting Information).

The growth of a single crystal from solution of **1** is thus not reliable as well as further characterization by X-ray diffraction. Compound **2** was fully characterized by ^{1}H and ^{13}C NMR analysis. The ^{1}H NMR (benzene-d_6, 25 °C) exhibits four singlets at 1.71, 1.67, 1.36, and 1.35 ppm for the ^{t}Bu groups, in agreement with lower symmetry of the pentacoordinate monoalkyl species. Two complex AB patterns for the methylene protons of the two different benzyl groups, namely the one migrated to the imine carbon (two doublets of doublets at 3.03 and 2.73 ppm; $^2J_{HH}$ = 12.3 Hz; $^3J_{HH}$ = 6.6 and 3.3 Hz) and the Zr−C*H*$_2$Ph (two doublets at 2.56 and 2.36 ppm; $^2J_{HH}$ = 10.5 Hz). A doublet of doublets at 4.71 ppm for the methine protons of the amide group and a doublet at 7.89 ppm (J = 1.8 Hz) for the imine proton were additionally detected. In the aromatic region, four signals at 7.81, 7.56, 7.31, and 7.13 ppm were assigned to not equivalent protons of the phenoxo groups. The stereoselective formation of **2** further confirms the proposed structure for **1**. Actually, the benzyl migration in the trans and cis-β forms of **1** would produce two diastereoisomers resulting (at least formally) from the attack of the two prochiral faces of the ligand or the formation of two Cα-amido carbons with opposite configurations.

To get more stable catalyst precursors, we synthesized the chloride analogue of **1** via metathesis of ZrCl$_4$(THF)$_2$ with the sodium salt of the preligand ^{t}Bu$_4$salcyenH$_2$. This reaction produced in toluene at room temperature a yellow microcrystalline solid exhibiting elemental analysis closely corresponding to that of the expected

Scheme 2

1 **2**

3a **3b**
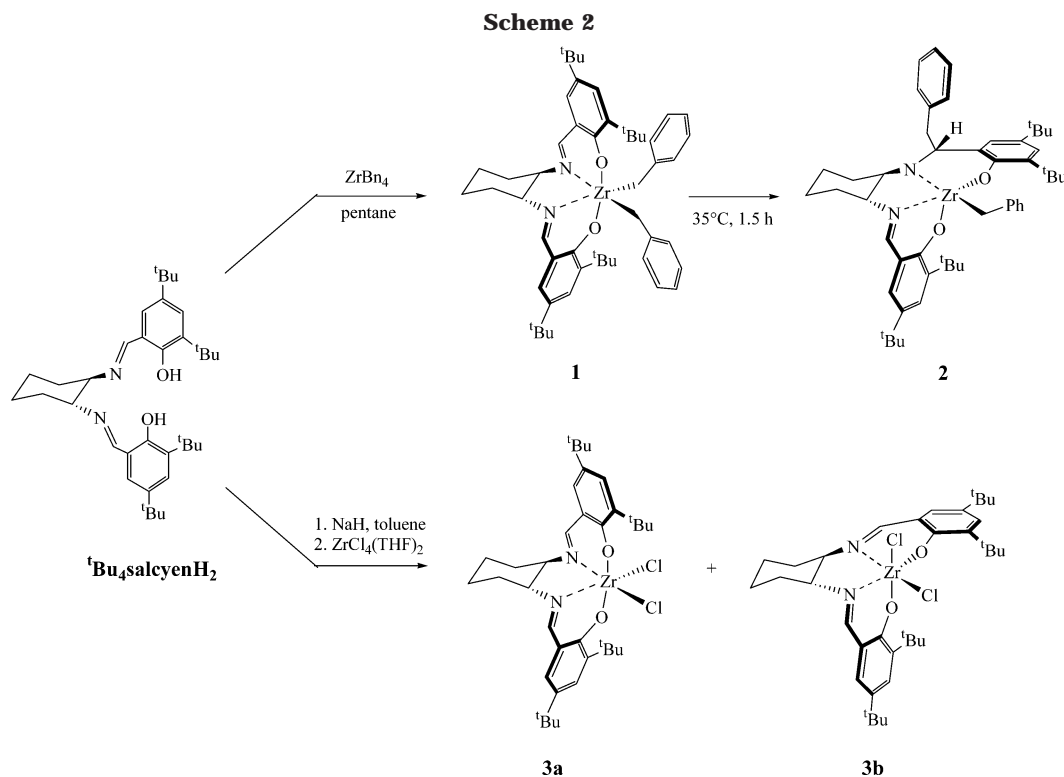
product. However, the ^{1}H NMR analysis revealed that the reaction mixture consists of two isomers of general formula [C$_6$H$_{10}$-{N=CH-(3,5-^{t}Bu$_2$C$_6$H$_2$-2-O)-κO}$_2$]ZrCl$_2$ [(^{t}Bu$_4$salcyen)ZrCl$_2$ (**3a,b**)] and structurally corresponding to the cis-α (**3a**) and cis-β (**3b**) in a 9:1 molar ratio (Scheme 2). The ^{1}H NMR spectrum (benzene-d_6, 25 °C) of the mixture exhibits a symmetric pattern for **3a** consisting of two singlets at 1.71 and 1.36 ppm for the ^{t}Bu groups and only one signal at 7.78 for the aldimino groups. An asymmetric pattern for **3b** containing four singlets at 1.76, 1.70, 1.31, and 1.29 ppm for the ^{t}Bu groups and two different signals at 7.77 and 7.68 ppm for the aldimino groups was additionally detected (see Figure 2). Attempts to synthesize **3** through different
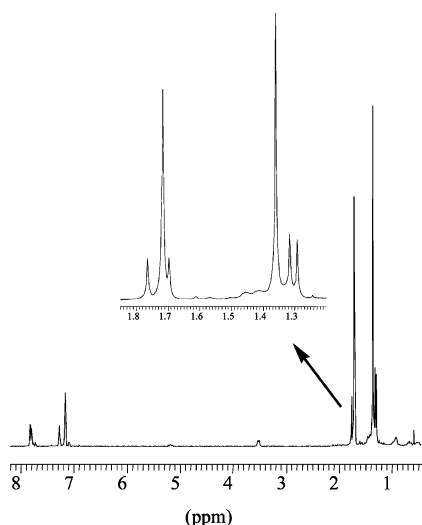
Figure 2. ^{1}H NMR spectrum (C$_6$D$_6$, 25 °C, δ in ppm) of (^{t}Bu$_4$salcyen)ZrCl$_2$ (**3**).

routes always produced the same mixture of **3a** and **3b** with the same relative ratio but in lower yields. For example, the reaction of the preligand with ZrCl$_4$(THF)$_2$

carried out in toluene at room temperature in the presence of triethylamine (Zr/N 1:2 molar ratio) produced **3a,b** (9:1 molar ratio) in 66% yield. The composition of the mixture of **3a** and **3b** resulted independent of the synthetic route used and even after repeated crystallizations in different solvents and conditions. Thus, we investigated by EXSY (exchange spectroscopy) NMR techniques the possibility that the cis-α and cis-β stereoisomers could be involved in an equilibrium reaction. Actually, the presence of EXSY correlation peaks found for the ^{t}Bu signals of the two stereoisomers suggested isomerization between this two forms with a kinetic rate of 3.6×10^{-1} s^{-1} (see Supporting Information).[31] We also investigated the behavior of the **3a,b** mixture by VT (variable temperature) ^{1}H NMR spectroscopy. At 100 °C in toluene the line width of the ^{t}Bu signals due to the cis-α form results little bit increased ($\Delta\nu_{1/2} = 2$ Hz), whereas the ^{t}Bu signals of the cis-β form reaches coalescence likely with trans stereoisomer. This suggests that the barrier to the conversion of the cis-α form with the other possible stereoisomers is higher than 84 kJ mol^{-1}. Fujita et al. reported on the basis of DFT calculations that the cis-α form of similar unbridged bis(iminophenolate) zirconium complex is more stable of about 20 kJ mol^{-1} and 33 kJ mol^{-1} than the cis-β and trans isomers, respectively.[25] Thus, it is not surprising the obtaining of a mixture of the two isomers **3a,b** with the most thermodynamically favored isomer largely prevailing. The stereoselective synthesis of **1** by protonolysis route could be likely favored by steric interaction of the bulky benzyl groups with the ^{t}Bu ortho substituents of the phenoxo groups.

2.2. Olefin Polymerization Catalyzed by 1 and 3. Activation of **1** with B(C$_6$F$_5$)$_3$, [CPh$_3$][B(C$_6$F$_5$)$_4$], or MAO produces active ethylene polymerization catalysts under a range of experimental conditions (see Table 1). The perfluoroborane is an activator less efficient than trityl salt and MAO (compare entries 2, 3, and 5), in agreement with previous reports on the polymerization

Table 1. Ethylene Polymerization Catalyzed by 1 and 3a,b

entry[a]	catalyst	cocatalyst	E (atm)	time (min)	yield (g)	activity[f]	M_w/M_n[g]	M_w ($\times 10^4$)
1[b]	**1**	$B(C_6F_5)_3/AlMe_3$	5	60	0.06	1.2		
2[b]	**1**	$B(C_6F_5)_3/Al\textit{i}Bu_3$	5	60	0.08	1.6	2.11	2
3[c]	**1**	$[CPh_3][B(C_6F_5)_4]/Al\textit{i}Bu_3$	5	60	0.80	16	1.64	280
4	**1**	MAO	5	100	13.0	156	2.52	22
5	**1**	MAO	5	60	6.30	126		
6	**1**	MAO	5	30	3.30	132		
7	**1**	MAO	5	6	0.98	196	1.53	218
8	**1**	MAO	5	3	0.30	120		
9[d]	**1**	MAO	1	60	0.47	9	1.84	109
10[c]	**3a,b**	$[CPh_3][B(C_6F_5)_4]/Al\textit{i}Bu_3$	5	60	0.30	6		
11	**3a,b**	MAO	5	60	2.85	57		
12	**3a,b**	$MAO/AlMe_3$	5	60	0.65	13		
13[e]	**3a,b**	MAO	1	60	0.62	62		
14[e]	**3a,b**	MAO	1	45	0.31	41	2.95	96
15[e]	**3a,b**	MAO	1	30	0.25	50	2.54	92
16[e]	**3a,b**	MAO	1	15	0.11	44	3.30	100

[a] Polymerization conditions: catalyst = 50 μmol ([Zr] = 5.0×10^{-4} M); toluene = 100 mL; Al/Zr molar ratio = 500; temperature = 30 °C. [b] B/Zr molar ratio = 1; Al/Zr molar ratio = 6. [c] B/Zr molar ratio = 1; Al/Zr molar ratio = 40. [d] Catalyst = 50 μmol ([Zr] = 1.0×10^{-3} M); toluene = 50 mL. [e] Catalyst = 10 μmol ([Zr] = 2.0×10^{-4} M); toluene = 50 mL. [f] Activity = g_{PE} $mmol_{cat}^{-1}$ h^{-1}. [g] Determined by GPC.

performances of the diaminobis(phenolate)benzylzirconium catalysts,[7] whereas the $[CPh_3][B(C_6F_5)_4]/Al$-$^iBu_3$ cocatalyst shows productivity values higher than former of nearly 1 order of magnitude. The use of trimethylaluminum as scavenger produces a decrease of the polymerization activity likely as a result of fast reaction with the imino functionality. Thus, solid MAO containing low amount of "*free*" (not coordinated) trimethylaluminum (see Experimental Section) was explored and found as the best activator (entries 4–9). Interestingly, the MAO activated catalyst is 8-fold more active than trityl activated catalyst (compare entries 3 and 5). A possible explanation is that the methyl cationic complex, resulting from reaction of **1** with MAO, is more thermally stable than the corresponding benzyl complex. Considering Scott's hypothesis of a fast benzyl vs alkyl migration from zirconium to the imino carbon of the ligand via radical mechanism,[30] this would produce a higher concentration of the active sites during the activation reaction. The polymerization activity of **1**/MAO increases almost linearly with polymerization time up to 100 min (entries 4–8). The polydispersity of the polyethylene samples produced with MAO and trityl activated catalysts (entries 3 and 7) is monomodal and narrow ($M_w/M_n < 2$), indicating the presence of a single active species. High molecular weights were found also at very short polymerization time.

The **3a,b** catalysts exhibits comparable performances. The activity of **3a,b**/MAO is lower than that found for **1** under the same conditions (compare entries 5 and 11) likely as a result, among other possible explanations, of precatalyst **3a,b** composition, isomerization between the cis-α and cis-β forms (where the latter is expected to be less active than former), and slow alkylation of the chloride derivatives followed with competitive decomposition of the active species. Addition of trimethylaluminum to solid MAO was found to produce a noxious effect (compare entries 11 and 12) analogously to the findings previously reported for the bis(iminophenolate)[24,32] and other nonmetallocene zirconium olefin polymerization catalysts.[33] The polymerization activity increases with polymerization time as long as 60 min, but the average molecular weights are nearly constant, indicating a fast chain transfer reaction with aluminum of MAO (entries 13–16). The $[CPh_3][B(C_6F_5)_4]/Al$-$^iBu_3$ cocatalyst resulted efficient in activating the chloride derivative (entry 10).
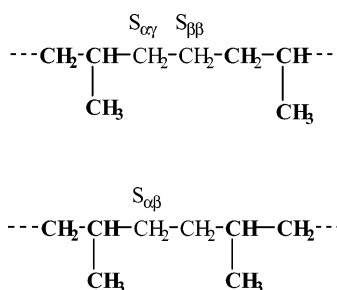
In all considered cases polyethylene produced is linear and exhibits melting points in the range 131–139 °C. Noteworthy the polydispersity index (PDI) of the polyethylene samples (PDI = 2.5–3.3) by **3a,b** is larger that than found with **1** although the propagating species during the polymerization catalyzed by these compounds are expected to be the same and the bulkiness of the growing polymer chain would hamper site isomerization between the C_2 to C_1 symmetric species during ethylene polymerization. The polymerization activity of **1** and **3a,b** dramatically decreases by passing from ethylene to propylene. This is not surprising considering data reported for the unbridged bis(iminophenolate) catalysts carrying not perfluorinated N-aromatic substituents[16,34] as well as the performances of the bis(amidinate)[6] and diaminobis(phenolate)[11] octahedral zirconium complexes in propylene polymerization. The reason probably arises from electronic properties of the metal center bearing this ligand. Traces of isotactic polypropylene were recovered from propylene polymerization experiments likely resulting from a minor organometallic species produced by the ligand leaching in the presence of high concentration of MAO: actually polypropylene with similar ^{13}C NMR fingerprints were produced by $ZrCl_4(THF)_2$/MAO under similar conditions.[33]

To gain information on the stereo- and regiochemistry of the propylene insertion, copolymerizations of ethylene with propylene were conducted under a range of experimental conditions in the presence of the bridged diiminobis(phenolate) complexes **1** and **3a,b**. The results are summarized in Table 2. Ethylene–propylene copolymers with propylene concentration up to 56 mol % were obtained. The copolymerization rate is rather low and decreases when propylene concentration in the feed is increased. The ^{13}C NMR analysis of the copolymer obtained in run 19 (P mol % = 43) revealed that the regiospecificity of the propylene insertion is highly primary because of the lacking of ^{13}C NMR signals in the region 35.7–34.9 ppm due to $S_{\alpha\beta}$ carbons.[35] Indeed, the secondary propylene insertion would produce a resting state of the catalyst which would favor ethylene insertion followed by primary propylene insertion. The sequence of these events produces a PEP triads which apparently corresponds to the tail-to-tail propylene enchainment of a PP diad characterized by the presence of the $S_{\alpha\beta}$ carbons shown in Scheme 3. Moreover, the

Table 2. Olefin Copolymerization Catalyzed by 1 and 3a,b Activated with MAO

entry[a]	catalyst	comonomer	comonomer concn in the feed (mol/L)	ethylene concn in the feed (mol/L)	time (h)	yield (g)	comonomer concn in the polymer (mol %)	M_w/M_n[f]	M_w ($\times 10^3$)
17	**1**	propene	0.6	0.005	1	0.26	19	2.2	63
18[b]	**1**	propene	1.3	0.013	1	0.06	26		
19[b]	**1**	propene	2.4	0.32	1	0.62	43	2.0	55
20[b]	**1**	propene	2.4	0.17	1	0.08	56		
21	**3a,b**	propene	0.5	0.005	1	0.07	10		
22[c]	**1**	1-hexene	3.2	0.20	3	2.56	12		
23[c]	**1**	1-hexene	6.4	0.20	3	2.74	33	2.1	81
24[d]	**1**	1-hexene	6.4	0.10	1	0.14	38		
25[e]	**1**	1-hexene	neat	0.20	3	0.33	22		
26[c]	**3a,b**	1-hexene	3.2	0.20	3	0.08	9	4.4	25

[a] Polymerization conditions: catalyst = 50 μmol ([Zr] = 1.0×10^{-3} M); Al/Zr molar ratio = 500; toluene = 50 mL; temperature = 25 °C. [b] Catalyst = 50 μmol ([Zr] = 5.0×10^{-4} M); toluene = 100 mL. [c] Toluene = 30 mL; 1-hexene = 20 mL. [d] Ethylene pressure = 0.5 atm. [e] 1-Hexene = 50 mL; cocatalyst = MMAO (7 wt % solution in heptane). [f] Determined by GPC.

Scheme 3

$S_{\alpha\gamma}$ $S_{\beta\beta}$
···CH₂–CH–CH₂–CH₂–CH₂–CH···
         | |
        CH₃   CH₃

$S_{\alpha\beta}$
···CH₂–CH–CH₂–CH₂–CH–CH₂···
         | |
   CH₃   CH₃

chemical shift of the $S_{\alpha\gamma}$ carbons of the PPEP tetrad is dramatically affected by the steric relationship between the two methyl groups of the propylene diad flanking ethylene. Actually the chemical shifts of the r-$S_{\alpha\gamma}$ and m-$S_{\alpha\gamma}$ carbons of the P^{r}PEP and P^{m}PEP tetrads fall at 38.8 and 37.9 ppm,[36] respectively, with the latter overlapping the resonance of the $S_{\alpha\gamma}$ of the EPEPE alternating pentad. In the ^{13}C NMR spectrum of sample 19 (Figure 3) two resonances due to the $S_{\alpha\alpha}$ carbons were
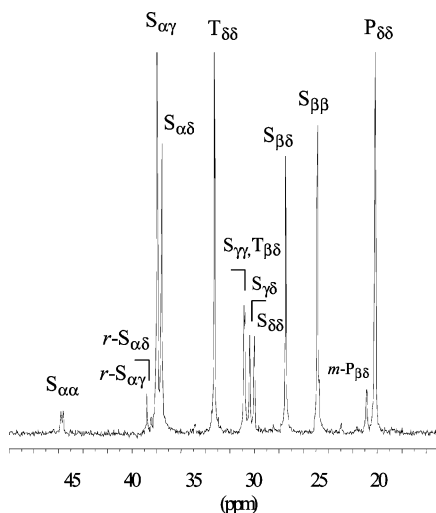
Figure 3. ^{13}C NMR spectrum (C₂D₂Cl₄, 110 °C, δ in ppm) of ethylene/propylene copolymer (entry 19, Table 2).

detected with the same intensity at 45.5 and 45.7 ppm and attributed to the PP diads with r and m stereochemistry.[35] The r-$S_{\alpha\gamma}$ signal is detected at 38.8 ppm with the expected 2:1 intensity ratio of r-$S_{\alpha\alpha}$. Noteworthy, the signal due to the m-$P_{\beta\delta}$ carbon is observed with the same intensity of r-$S_{\alpha\gamma}$ at 20.8 ppm. Considering that the signal of r-$P_{\beta\delta}$ would overlap the signal of $P_{\delta\delta}$ at 20.1 ppm and that of m-$S_{\alpha\gamma}$ overlaps that

of $S_{\alpha\gamma}$ of the EPEPE, this picture suggests aspecific propylene insertion, producing m- and r-PP diads completely at random. Moreover, in the ^{13}C NMR spectrum of the sample 20 (P mol % = 56) PPP triads were produced, and two more signals with the same intensity at 38.9 and 38.7 ppm were detected and attributed to the $S_{\alpha\gamma}$ of the P^{r}P^{r}PEP and P^{m}P^{r}PEP pentad (Figure 4). This finding confirms the lack of any
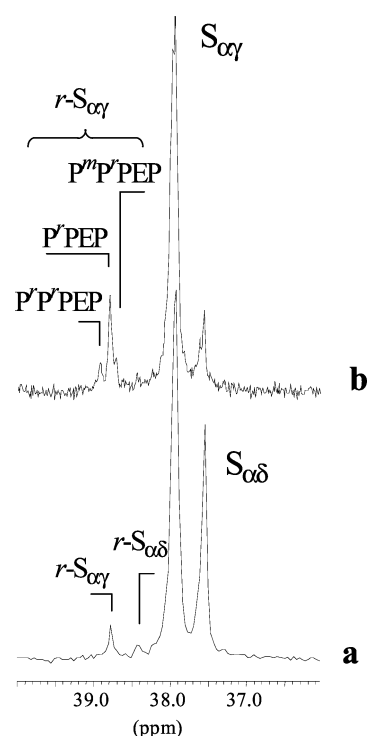
Figure 4. ^{13}C NMR spectral region (C₂D₂Cl₄, 110 °C, δ in ppm) of $S_{\alpha\gamma}$: (a) P mol % = 43 (run 19, Table 2) and (b) P mol % = 56 (run 20, Table 2).

stereocontrol in the formation of propylene homosequences. Unfortunately, the check for the same splitting for the P^{r}P^{m}PEP and P^{m}P^{m}PEP pentads is not possible for the overlap of these resonances with that of $S_{\alpha\gamma}$ of EPEPE at 37.8 ppm.

Aiming to obtain copolymers with higher 1-olefins and get information on their microstructure, copolymerization of ethylene with 1-hexene was carried out using the **1** and **3** catalysts. Ethylene-*co*-1-hexene polymers with 1-hexene concentration up to 38 mol % were obtained (entry 24, Table 2). Copolymerization runs carried out in neat 1-hexene using MMAO cocatalyst

to prevent catalyst precipitation yielded copolymers with lower incorporation of 1-hexene (entry 25, Table 2). ^{13}C NMR analysis of the copolymer microstructure of sample 23 suggested that 1-hexene was mainly incorporated as isolated units producing ^{13}C NMR signals at 38.1 and 34.5 ppm attributed to the methine and methylene ($S_{\alpha\delta+}$) of the main-chain carbons, respectively, and signals at 34.1, 29.3, 23.4, and 14.3 ppm attributed to the carbon atoms in the butyl branch (see Supporting Information). However, additional signals at 35.0 and 24.5 ppm were attributed to $S_{\alpha\gamma}$ and $S_{\beta\beta}$ carbons of alternating triad HEH.[40] In the ^{13}C NMR spectrum of sample 26, signals due to the HH diads were detected with very low intensity, but unfortunately no conclusion on the stereochemistry of 1-hexene insertion could be reached. Noteworthy, the gel permeation chromatography (GPC) curve of the ethylene−1-hexene and ethylene−propylene copolymers is monomodal and the PDI is close to 2, comparable to that found for polyethylene, indicating the homogeneity of the copolymers and that they result from a single catalytic species.

The results herein reported for the stereo- and regiochemistry of 1-olefin insertion with bridged diiminobis-(phenolate) catalysts **1** and **3** are in qualitative agreement with experimental data reported for the corresponding unbridged zirconium complexes. However, the bridged catalysts exhibit higher regiospecificity, and propylene insertion occurs exclusively in a primary fashion. Despite the C_2 symmetry of the **1** and **3** catalyst the stereochemistry of propylene insertion is aspecific, indicating that both ligand environment and chirality of the last unit in the growing polymer chain are unable to express face selectivity in the monomer coordination/insertion likely as a result of a too large mouth of the catalyst and the distance of the chiral methine of the growing polymer chain from the metal of the active species. Thus, the regiospecificity of the propylene insertion seems mainly due to electronic factors and not to the steric hindrance at the metal center.

The fluxional behavior of the unbridged bis(iminophenolate) catalysts could explain the higher polymerization activity of these complexes in propylene polymerization compared to that of the title catalysts.

3. Conclusions

We reported the synthesis and characterization of diiminobis(phenolate) zirconium complexes [C$_6$H$_{10}$-{N= CH-(3,5-*t*Bu$_2$C$_6$H$_2$-2-O)-κO}$_2$]ZrX$_2$ [X = CH$_2$Ph (**1**), Cl (**3**)]. The chloride derivative is thermally stable and found in slow equilibrium between the cis-α and cis-β forms with the former largely prevalent (9:1 molar ratio). The kinetic barrier to the isomerization has been estimated higher than 84 kJ mol^{-1} by NMR methods, and the kinetic constant for the interconversion between the two diastereisomers is 3.6×10^{-1} s^{-1}. The corresponding benzyl zirconium complex is conformationally more stable and pure and has been isolated with C_2 symmetry. Thus, the steric interaction between the zirconium ancillary ligands and the ortho substituent at the aryloxo groups bound to zirconium plays a relevant role in stabilizing the C_2 symmetry of this zirconium complex. Assuming that the growing polymer chain is a sterically demanding group, the C_2 symmetry of the catalyst would further be stabilized by the presence of this bulky group bound to the metal of the active center and retained during polymerization. The benzyl complex **1** is light sensitive and readily under-

goes to 1,2 benzyl migration from the metal to the imino carbon, converting the diiminobis(phenolate) ligand in the corresponding benzylamidoiminobis(phenolate). This decomposition pathway reduces the number of the active sites and the polymerization activity as a consequence. When complexes **1** and **3** were activated with MAO, ethylene polymerization catalysts with moderate activity were found: the polydispersity of the polyethylene samples obtained in a range of experimental conditions is monomodal and close to 2, suggesting the presence of a single active species. The catalyst is stable over 3 h, and the polymerization activity linearly increases with time. The ligand leaching can be ruled out because the ZrCl$_4$(THF)$_2$/MAO catalyst produces polyethylenes with broader molecular weight distribution (PDI > 5) under comparable conditions.[33] Ethylene−1-olefin copolymerization experiments confirmed the stereo- and regiochemistry of 1-olefin insertion previously reported for the corresponding unbridged complexes. The regiospecificity is highly primary, but stereospecificity is scarce because of inefficient control of the ligand framework and low steric interaction of the coordinated monomer with the chiral methine of the last unit in the growing polymer chain.

4. Experimental Section

4.1. General Information. All organic preparations were carried out under normal atmospheric conditions, while organometallic manipulations were performed under a dry nitrogen atmosphere using standard Schlenk line techniques and a glovebox. Solvents (toluene, hexane, pentane, tetrahydrofuran) were refluxed and distilled over sodium benzophenone before use. (1*R*,2*R*)-Cyclohexanediamine, 3,5-di-*tert*-butyl-2-hydroxybenzaldehyde, HCOOH, *n*-BuLi, ZrCl$_4$, NaH, AlMe$_3$, Al*i*Bu$_3$ (Aldrich), [CPh$_3$][B(C$_6$F$_5$)$_4$] (Boulder SPA Co.), and B(C$_6$F$_5$)$_3$ (Strem Chemicals) were used as received. Triethylamine and 1-hexene (Aldrich) were distilled from CaH$_2$. Ethylene and propylene (S.O.N., polymerization grade) were dried by passing over activated 4 Å molecular sieves. Methylalumoxane (MAO) (Witco, 10 wt % solution in toluene) was dried in a vacuum at 50 °C to remove the uncoordinated AlMe$_3$ and used as a solid after washing hexane. Modified methylalumoxane (MMAO-3A) (Akzo Nobel, 7 wt % solution in heptane) was used as received. ZrBn$_4$[37] and ZrCl$_4$(THF)$_2$[38] were prepared according to the literature procedures. Elemental analyses were performed with a Perkin-Elmer 240-C instrument.

4.2. Synthesis of *N,N*-(1*R*,2*R*)-Cyclohexylenebis(3,5-di-*tert*-butylsalicylidene imine) (*t*Bu$_4$salcyenH$_2$). The preligand *t*Bu$_4$salcyenH$_2$ was readily synthesized by a modified literature procedure.[26,27] To a solution of 3,5-di-*tert*-butyl-2-hydroxybenzaldehyde (10.75 g, 0.46 mmol) in methanol (240 mL) 0.3 mL of formic acid was added under stirring followed by the addition of a solution of (1*R*,2*R*)-cyclohexanediamine (2.62 g, 23 mmol) in methanol (20 mL). The resulting mixture was dilute with methanol to reach a total volume of 400 mL and stirred overnight at room temperature. A yellow precipitate was recovered by filtration. Further crops were collected by crystallization of the mother liquor at −10 °C. The yellow solid was dried overnight in a vacuum at 65 °C (11.0 g, yield 88%).

4.3. Syntheses of 1, 2, and 3a,b. 4.3.1. Synthesis of (*t*Bu$_4$salcyen)ZrBn$_2$ (1). A yellow solution of the *t*Bu$_4$-salcyenH$_2$ (1.0 g, 1.83 mmol) in pentane (60 mL) was added dropwise to a stirred suspension of ZrBn$_4$ (0.84 g, 1.83 mmol) in pentane (20 mL) for 10 min at room temperature, affording a red solution. Quick removal of the solvent in a vacuum gave the expected product as a red-orange powder (1.4 g, 1.77 mmol, yield 93%).

^{1}H NMR data (C$_6$D$_6$, 25 °C, δ in ppm): δ 8.04 (s, 2H, C*H*= N), 7.92 (d, 2H, J = 2.4 Hz, Ar*H*), 7.39 (d, 2H, J = 2.4 Hz, Ar*H*), 6.63 (t, 4H, *m*-Ph), 6.52 (t, 2H, *p*-Ph), 6.45 (d, 4H, *o*-Ph), 2.77−2.70 (AB pattern, 4H, ^2J = 7.6 Hz, C*H$_2$*Ph), 2.18 (br, 2H,

cyclohexyl C*H*), 1.85 (s, 18H, *t*Bu), 1.41 (s, 18H, *t*Bu), other cyclohexyl resonances obscured. ^{13}C NMR (C_6D_6, 25 °C, δ in ppm): δ 163.7 (*C*H=N), 162.1 (*C*−O), 145.4 (*C*−CH=N), 139.7, 139.3, 131.1, 130.9, 128.5 (Ar), 125.6, 124.5, 120.5 (Ph), 72.3 (cyclohexyl *C*H), 67.0 (*C*H$_2$Ph), 35.9, 34.4 (*C*Me$_3$), 31.7, 30.54 (C(*C*H$_3$)$_3$), 29.4, 24.6 (cyclohexyl *C*H$_2$).

Anal. Found: C, 73.02; H, 8.71; N, 3.67. Calcd for $C_{50}H_{66}N_2O_2$-Zr: C, 73.3; H, 8.13; N, 3.42.

4.3.2. Synthesis of (Bn*t*Bu$_4$salcyen)ZrBn (2). A red solution of benzyl complex **1** (0.11 g, 0.13 mmol) in toluene (8 mL) was stirred for 1.5 h at 35 °C, during which time the solution slowly turned red/yellow. Distilling off the solvent in a vacuum, a glassy yellow solid was obtained (0.09 g, 0.11 mmol, yield 82%).

^{1}H NMR data (C_6D_6, 25 °C, δ in ppm): δ 7.89 (d, 1H, J = 1.8 Hz, C*H*=N), 7.81 (d, 1H, J = 1.7 Hz, Ar*H*), 7.56 (d, 1H, J = 2.4 Hz, Ar*H*), 7.31 (d, 1H, J = 1.7 Hz, Ar*H*), 7.13 (d, 1H, J = 2.4 Hz, Ar*H*), 7.02 (m, 2H, *m*-Ph), 6.84 (m, 1H, *p*-Ph), 6.78 (m, 4H, *m′*-Ph and *o*-Ph), 6.63 (t, 1H, *p′*-Ph), 6.55 (d, 2H, *o′*-Ph), 4.71 (dd, 1H, ^3J = 6.6 and 3.3 Hz, N−C*H*) 3.03−2.73 (dd, 2H, AB pattern, ^2J = 12.3 Hz, ^3J = 6.6 and 3.3 Hz, C*H*$_2$Ph migrated to the imine carbon), 2.56−2.36 (d, 2H, AB pattern, ^2J = 10.5 Hz, Zr−C*H*$_2$Ph), 2.28 (br, 1H, cyclohexyl C*H*N=C), 1.71, 1.67, 1.36, 1.35 (s, 9H, *t*Bu). ^{13}C NMR (C_6D_6, 25°C, δ in ppm): δ 160.5 (*C*H=N), 159.8 (*C*−O), 154.8 (*C*−O), 146.1 (*C*−CH=N), 141.3 (*C*−CH=N), 141.1, 139.6, 136.9, 133.4, 130.3, 129.2 (Ar), 129.1, 128.9, 127.4, 125.1(Ph), 122.9, 120.9 (Ar), 69.8, 69.4 (cyclohexyl *C*H), 67.3, 58.4 (*C*H$_2$Ph), 41.0 (*C*H−N), 35.73 (*C*Me$_3$), 32.0 (C(*C*H$_3$)$_3$), 31.8 (*C*Me$_3$), 31.6 (C(*C*H$_3$)$_3$), 30.8, 30.7 (*C*Me$_3$), 30.4, 30.2 (C(*C*H$_3$)$_3$), 27.1, 25.3, 25.1, 23.0 (cyclohexyl *C*H$_2$).

Anal. Found: C, 73.02; H, 8.25; N, 3.40. Calcd for $C_{50}H_{66}N_2O_2$-Zr: C, 73.3; H, 8.13; N, 3.42.

4.3.3. Synthesis of (*t*Bu$_4$salcyen)ZrCl$_2$ (3a,b). The synthesis of the complex **3a,b** was carried out by two different routes.

Method A. A toluenic solution (10 mL) of *t*Bu$_4$salcyenH$_2$ (0.40 g, 0.73 mmol) and NEt$_3$ (0.20 mL, 1.5 mmol) was added to a stirred suspension of ZrCl$_4$(THF)$_2$ (0.28 g, 0.74 mmol) in toluene (10 mL). The mixture was stirred at room temperature overnight. The yellow solution was filtered, and the yellow solid was isolated after distillation of the solvent. The solid was washed with hexane and dried in a vacuum (0.34 g, 0.48 mmol, yield 66%).

Method B. To a solution of *t*Bu$_4$salcyenH$_2$ (0.61 g, 1.11 mmol) in toluene (25 mL) solid NaH (0.06 g, 2.5 mmol) was added under nitrogen, and the resulting mixture was stirred overnight at room temperature. The yellow suspension of the sodium salt Na$_2$*t*Bu$_4$salcyen was added dropwise to a suspension of ZrCl$_4$(THF)$_2$ (0.42 g, 1.11 mmol) in toluene (20 mL) and stirred for 12 h. The reaction mixture was filtered and the expected product was isolated by crystallization in toluene at 4 °C as yellow solid (0.75 g, 1.1 mmol, yield 96%).

^{1}H NMR data (C_6D_6, 25 °C, δ in ppm) for **3a**: δ 7.82 (d, 2H, J = 2.3 Hz, Ar*H*), 7.78 (s, 2H, C*H*=N), 7.26 (d, 2H, J = 2.3 Hz, Ar*H*), 3.53 (m, 2H, cyclohexyl C*H*), 1.71 (s, 18H, *t*Bu), 1.36 (s, 18H, *t*Bu), 0.70 (m, 4H, cyclohexyl C*H*$_2$), 0.53 (m, 4H, cyclohexyl C*H*$_2$). For **3b**: δ 7.77, 7.68 (s, 1H, C*H*=N), 7.24 (d, 2H, J = 2.6 Hz, Ar*H*), 7.08 (d, 2H, J = 2.5 Hz, Ar*H*), 1.76, 1.70, 1.31, 1.29 (s, 9H, *t*Bu). ^{13}C NMR (C_6D_6, 25 °C, δ in ppm) for **3a**: δ 165.5 (*C*H=N), 160.0 (*C*−O), 142.3 (*C*−C=N), 139.7, 132.5, 131.3, 124.8 (Ar), 67.5 (cyclohexyl *C*H), 36.2, 34.8 (*C*Me$_3$), 31.9, 30.5 (C(*C*H$_3$)$_3$), 28.0, 24.3 (cyclohexyl *C*H$_2$). Anal. Found: C, 61.45; H, 7.63; N, 3.93. Calcd for $C_{36}H_{52}Cl_2N_2O_2$Zr: C, 61.16; H, 7.41; N, 3.96.

4.4. Polymerization Procedure. The polymerization runs were carried out following a standard procedure. A sealed glass vial containing the appropriate amount of precatalyst was introduced into a 500 mL Bücki glass autoclave equipped with a mechanical stirrer. The autoclave was evacuated and charged with the desired amount of alkylaluminum compound dissolved in toluene. After the equilibration of the solution with ethylene or propylene at the appropriate pressure and temperature, the polymerization run was started by breaking the vial with the mechanical stirrer. The run was terminated by

venting the reaction vessel and pouring the polymerization mixture into ethanol acidified with aqueous HCl. The coagulated polymer was recovered by filtration, washed with an excess of fresh ethanol, and dried in a vacuum at room temperature. The polymerization runs with monomer fed at atmospheric pressure were performed by introducing toluene and the alkylaluminum reagent into a 100 mL flask equipped with a magnetic bar. The nitrogen atmosphere was replaced with ethylene, and the polymerization run was started after equilibration of the solution with ethylene at the desired temperature by injection of a solution of the precatalyst in toluene.

Copolymerization Procedure. Copolymerizations of ethylene with propylene were performed following the procedures above-described, the only difference being the feeding of the reactor. In entries 17 and 21, ethylene and propylene were mixed at atmospheric pressure with appropriate compositions using a Brooks gas flowmeter, and the gas phase let flow through the polymerization solution with a rate of 500 mL/min. The inlet and outlet gas-phase compositions were monitored by gas chromatography analysis. In entries 18−20, 25 mL of propylene was condensed in the toluene solution containing MAO, and thus ethylene was fed at 1.3 (entry 19) and 0.7 atm (entry 20).

Copolymerizations of ethylene with 1-hexene were performed in a 100 mL flask equipped with a magnetic stir bar. The glass reactor was charged with toluene, 1-hexene, and MAO in that order, and the nitrogen atmosphere was replaced with ethylene fed at atmospheric pressure. When the solution reached thermodynamic equilibrium with the gas phase, the reaction was started by injection of a toluene solution of the precatalyst. The polymerization run was stopped by addition of ethanol acidified with aqueous HCl and the copolymers isolated according to the conventional procedure.

Characterization of the Polymers. *NMR Characterization.* ^{1}H and ^{13}C NMR spectra of the organometallic compounds were recorded with a Bruker ADVANCE 400 spectrometer (400 MHz for ^{1}H and 100 MHz for ^{13}C). The ^{13}C NMR spectra of the polymer and copolymer samples were recorded with an AM 250 Bruker spectrometer (250 MHz for ^{1}H and 63 MHz for ^{13}C) at 110 °C using 1,1,2,2-tetrachloroethane-d_2 as solvent (0.5 mL, 20 wt %). The ^{1}H NMR chemical shifts were referred to TMS as external standard using the residual protio impurities of the deuterated solvents as reference. The ^{13}C NMR chemical shifts were calibrated using the $S_{δδ}$ signal of polyethylene at 30.0 ppm as internal reference. The copolymer compositions were estimated using the method proposed in the literature.[35,39,40]

GPC analysis of the polymers was carried out by high-temperature GPC at 140 °C using 1,2,4-trichlorobenzene as solvent and narrow MWD polystyrene standard sample as reference. The measurements were performed on a PL-GPC210 with four PL-Gel Mixed A columns, RALLS (light scattering) detector (PD2040), H502 viscometer (Viscotek), refractive detector, and DM400 data manager (Viscotek).

Differential scanning calorimetry (DSC) measurements were carried out with a TA Instrument DSC 2920 at a heating rate of 10 °C/min.

Supporting Information Available: Kinetic study of thermal decomposition of complex **1**, EXSY NMR spectrum of complex **3**, and ^{13}C NMR spectrum of the ethylene-*co*-1-hexene

polymer (entry 25, Table 2). This material is available free of charge via the Internet at http://pubs.acs.org.

References and Notes

(1) Bochmann, M. *J. Chem. Soc., Dalton Trans.* **1996**, 255.
(2) Brintzinger, H.-H.; Fischer, D.; Mülhaupt, R.; Rieger, B.; Waymouth, R. M. *Angew. Chem., Int. Ed. Engl.* **1995**, *34*, 1143.
(3) Marks, T. J. *Acc. Chem. Res.* **1992**, *25*, 57.
(4) Coates, G. W. *Chem. Rev.* **2000**, *100*, 1223.
(5) Volkis, V.; Shmulinson, M.; Averbuj, C.; Lisovskii, A.; Edelmann, F. T.; Eisen, M. S. *Organometallics* **1998**, *17*, 3155.
(6) Volkis, V.; Nelkenbaum, E.; Lisovskii, A.; Hasson, G.; Semiat, R.; Kapon, M.; Botoshansky, M.; Eishen, Y.; Eisen, M. S. *J. Am. Chem. Soc.* **2003**, *125*, 2179.
(7) Tshuva, E. Y.; Goldberg, I.; Kol, M. *J. Am. Chem. Soc.* **2000**, *122*, 10706.
(8) Tshuva, E. Y.; Goldberg, I.; Kol, M.; Goldschmidt, Z. *Inorg. Chem. Commun.* **2000**, 611.
(9) Tshuva, E. Y.; Goldberg, I.; Kol, M.; Goldschmidt, Z. *Organometallics* **2001**, *20*, 3017.
(10) Tshuva, E. Y.; Goldberg, I.; Kol, M.; Goldschmidt, Z. *Chem. Commun.* **2001**, 2120.
(11) Busico, V.; Cipullo, R.; Ronca, S.; Budzelaar, P. H. M. *Macromol. Rapid Commun.* **2001**, *22*, 1405.
(12) Matsui, S.; Mitani, M.; Saito, J.; Matsukawa, N.; Tanaka, H.; Nakano, T.; Fujita, T. *Chem. Lett.* **2000**, 554.
(13) Matsui, S.; Mitani, M.; Saito, J.; Tohi, Y.; Makio, H.; Matsukawa, N.; Takagi, Y.; Tsuru, K.; Nitabaru, M.; Nakano, T.; Tanaka, H.; Kashiwa, N.; Fujita, T. *J. Am. Chem. Soc.* **2001**, *123*, 6847.
(14) Saito, J.; Mitani, M.; Mohri, J.-I.; Yoshida, Y.; Matsui, S.; Ishii, S.-I.; Kojoh, S.-I.; Kashiwa, N.; Fujita, T. *Angew. Chem., Int. Ed.* **2001**, *40*, 2918.
(15) Suzuki, Y.; Terao, H.; Fujita, T. *Bull. Chem. Soc. Jpn.* **2003**, *76*, 1493.
(16) Tian, J.; Coates, G. W. *Angew. Chem., Int. Ed.* **2000**, *39*, 3626.
(17) Saito, J.; Mitani, M.; Onda, M.; Mohri, J.-I.; Ishii, S.-I.; Yoshida, Y.; Nakano, T.; Tanaka, H.; Matsugi, T.; Kojoh, S.-I.; Kashiwa, N.; Fujita, T. *Macromol. Rapid Commun.* **2001**, *22*, 1072.
(18) Mitani, M.; Furuyama, R.; Mohri, J.-I.; Saito, J.; Ishii, S.; Terao, H.; Nakano, T.; Tanaka, H.; Fujita, T. *J. Am. Chem. Soc.* **2003**, *125*, 4293.
(19) Mitani, M.; Furuyama, R.; Mohri, J.-I.; Saito, J.; Ishii, S.; Terao, H.; Kashiwa, N.; Fujita, T. *J. Am. Chem. Soc.* **2002**, *124*, 7888.
(20) Ishii, S.-I.; Furuyama, R.; Matsukawa, N.; Saito, J.; Mitani, M.; Tanaka, H.; Fujita, T. *Macromol. Rapid Commun.* **2003**, *24*, 452.
(21) Lamberti, M.; Pappalardo, D.; Zambelli, A.; Pellecchia, C. *Macromolecules* **2002**, *35*, 658.
(22) Milano, G.; Cavallo, L.; Guerra, G. *J. Am. Chem. Soc.* **2002**, *124*, 13368.
(23) Talarico, G.; Busico, V.; Cavallo, L. *J. Am. Chem. Soc.* **2003**, *125*, 7172.
(24) Lamberti, M.; Gliubizzi, R.; Mazzeo, M.; Tedesco, C.; Pellecchia, C. *Macromolecules* **2004**, *37*, 276.
(25) Tohi, Y.; Makio, H.; Matsui, S.; Onda, M.; Fujita, T. *Macromolecules* **2003**, *36*, 523.
(26) Belokon, Y.; Ikonnikov, N.; Moscalenko, M.; North, M.; Orlova, S.; Tararov, V.; Yashkina, L. *Tetrahedron: Asymmetry* **1996**, *7*, 851.
(27) Larrow, J. F.; Jacobsen, E. N.; Gao, Y.; Hong, Y.; Nie, X.; Zepp, C. M. *J. Org. Chem.* **1994**, *59*, 1939.
(28) Floriani, C.; Solari, E.; Corazza, F.; Chiesi-Villa, A.; Guastini, C. *Angew. Chem., Int. Ed. Engl.* **1989**, *28*, 64.
(29) Woodman, P. R.; Alcock, N. W.; Munslow, I. J.; Sanders, C. J.; Scott, P. *J. Chem. Soc., Dalton Trans.* **2000**, 3340.
(30) Knight, P. D.; Clarke, A. J.; Kimberley, B. S.; Jackson, R. A.; Scott, P. *Chem. Commun.* **2002**, 352.
(31) Perrin, C. L.; Dwyer, T. J. *Chem. Rev.* **1990**, *90*, 935.
(32) Saito, J.; Onda, M.; Matsui, S.; Mitani, M.; Furuyama, R.; Tanaka, H.; Fujita, T. *Macromol. Rapid Commun.* **2002**, *23*, 1118.
(33) Proto, A.; Capacchione, C.; Motta, O.; De Carlo, F. *Macromolecules* **2003**, *36*, 5942.
(34) Tian, J.; Hustad, P. D.; Coates, G. W. *J. Am. Chem. Soc.* **2001**, *123*, 5134.
(35) Cheng, H. N. *Macromolecules* **1984**, *17*, 1950.
(36) Hayashi, T.; Inoue, Y.; Chûjô, R.; Asakura, T. *Polymer* **1988**, *29*, 2208.
(37) Zucchini, U.; Albizzati, E.; Giannini, U. *J. Organomet. Chem.* **1971**, *26*, 357.
(38) Manzer, L. E. *Inorg. Synth.* **1982**, *21*, 135.
(39) De Pooter, M.; Smith, P. B.; Dohrer, K. K.; Bennet, K. F.; Meadows, M. D.; Smith, C. G.; Schouwenaars, H. P.; Geerards, R. A. *J. Appl. Polym. Sci.* **1991**, *42*, 399.
(40) Randall, J. C. *Rev. Macromol. Chem. Phys.* **1989**, *C29*, 201.